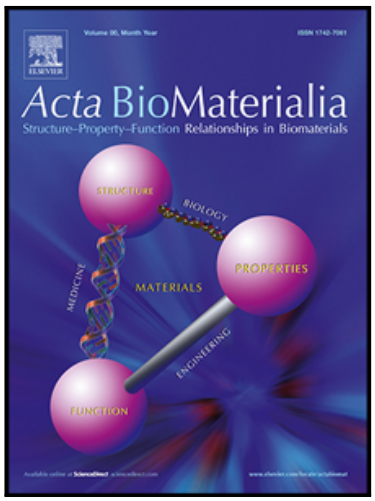
Journal Pre-proof



Co-localization and crosstalk between CD44 and RHAMM depend on hyaluronan presentation

Ana M. Carvalho , Diana Soares da Costa , Pedro M.R. Paulo , Rui L. Reis , Iva Pashkuleva

PII: S1742-7061(20)30613-9
DOI: https://doi.org/10.1016/j.actbio.2020.10.024
Reference: ACTBIO 6996

To appear in: *Acta Biomaterialia*

Received date: 14 May 2020
Revised date: 9 October 2020
Accepted date: 13 October 2020

Please cite this article as: Ana M. Carvalho , Diana Soares da Costa , Pedro M.R. Paulo , Rui L. Reis , Iva Pashkuleva , Co-localization and crosstalk between CD44 and RHAMM depend on hyaluronan presentation, *Acta Biomaterialia* (2020), doi: https://doi.org/10.1016/j.actbio.2020.10.024

This is a PDF file of an article that has undergone enhancements after acceptance, such as the addition of a cover page and metadata, and formatting for readability, but it is not yet the definitive version of record. This version will undergo additional copyediting, typesetting and review before it is published in its final form, but we are providing this version to give early visibility of the article. Please note that, during the production process, errors may be discovered which could affect the content, and all legal disclaimers that apply to the journal pertain.

© 2020 Published by Elsevier Ltd on behalf of Acta Materialia Inc.

Journal Pre-proof

Co-localization and crosstalk between CD44 and RHAMM depend on hyaluronan presentation

Ana M. Carvalho[1,2], Diana Soares da Costa[1,2], Pedro M. R. Paulo[3], Rui L. Reis[1,2], Iva Pashkuleva[1,2*]*

[1] 3B's Research Group – Biomaterials, Biodegradable and Biomimetics, Avepark - Parque de Ciência e Tecnologia Zona Industrial da Gandra 4805-017 Barco GMR – Portugal; [2] ICVS/3B's – PT Government Associate Laboratory, University of Minho, Portugal; [3] Centro de Química Estrutural, Instituto Superior Técnico, Universidade de Lisboa, Av. Rovisco Pais 1, 1049-001 Lisboa, Portugal

* ammpfc@i3bs.uminho.pt; pashkuleva@i3bs.uminho.pt

Abstract: CD44 and the receptor for hyaluronic acid-mediated motility (RHAMM) are the main hyaluronan (HA) receptors. They are commonly overexpressed in different cancers activating signaling pathways related to tumor progression, metastasis and chemoresistance. Besides their involvement in signal transduction *via* interaction with HA, currently, there is a little information about the possible crosstalk between CD44 and RHAMM and the role of HA in this process. In the present work, we used immunocytochemistry combined with Förster resonance energy transfer (FRET) microscopy and co-immunoprecipitation to elucidate the involvement of HA in CD44 and RHAMM expression, co-localization and crosstalk. We studied breast cancer cells lines with different degrees of invasiveness and expression of these receptors in the absence of exogenous HA and compared the data with the results obtained for cultures supplemented with either soluble HA or seeded on substrates with end-on immobilized HA. Our results demonstrated that cells response depends on the HA presentation: CD44/RHAMM complexation was upregulated in all cell lines upon interaction with immobilized HA, but not with its soluble form. Moreover, the results showed that the expression of both CD44 and RHAMM is regulated *via* interactions with HA indicating cell-specific feedback loop(s) in the signaling cascade.

Keywords: Breast cancer; CD44; RHAMM; Hyaluronan; FRET

1. Introduction

Hyaluronan (HA) is a linear non-sulfated glycosaminoglycan synthesized at the cell surface and secreted into the extracellular environment. Once secreted, HA assembles with different components of the extracellular matrix (ECM) and interacts with cell receptors, thus, mediating both ECM-cell and cell-cell crosstalk.[1-5] HA is critical in various physiological processes and its amount is tightly controlled and regulated by several HA synthetases (HAS) and hyaluronidases (HYAL).[6-9] The expression of these enzymes is altered in different pathological states, *e.g.* cancers and inflammation, causing specific HA turnover profile.[6, 9-13] Overexpression of HAS (mainly HAS2 but also HAS1 and HAS3) is a hallmark of several malignancies and related with poor prognosis: it results in accumulation of HA both in tumor parenchyma and in the surrounding stroma.[14-18] The molecular size of the accumulated HA is also altered: the proportion of short fragments is greater due to the HYALs and reactive oxygen species (ROS), which are overexpressed in tumor microenvironment.[6, 9, 19] These HA changes trigger different cell behavior (*e.g.* increased cell survival, drug resistance, proliferation, migration/motility, invasion and metastasis) by the formation of immunoprotective pericellular coats and through interactions of the generated HA fragments with the cellular receptors.[18-22]

There are two main HA receptors – the transmembrane glycoprotein CD44 and the receptor for HA-mediated motility (RHAMM). The standard form of CD44 (CD44s) is widely expressed in cells of different healthy tissues. Inflammation and several types of cancer are associated with upregulation and structural changes of the extracellular domain of CD44, giving rise to so-called variants (CD44v) that promote tumor progression and metastasis.[23-25] CD44 binds HA *via* an amino-terminal link domain leading to ligand-induced clustering of CD44.[26, 27] Of note, CD44 also binds other ECM components and is a co-receptor for different proteins, thus it is very sensitive to its environment and involved in the activation of several signaling pathways (e.g. Erk1/2, AKT and FAK).[1, 28-31] The minimal size of HA fragments that CD44 can bind is six monosaccharide units, *i.e.* the fragments generated by overexpressed HYAL in tumors still can bind to CD44 but clustering occurs only upon binding of oligosaccharides that are larger than 20 residues.[32-34] The interactions of HA with CD44 promote cell survival, motility and invasion.[20, 23, 25, 35]

RHAMM (also known as CD168 and hyaluronan-mediated motility receptor, HMMR) is a soluble protein with low or no expression in homeostatic tissues.[36, 37] It is an unusual protein:

structurally RHAMM is a typical cytoplasmic protein as it lacks a membrane-spanning domain and signal peptides needed for export via the Golgi/endoplasmic reticulum pathway.[38-40] Indeed, RHAMM is identified in the cytoplasm but also in the cytoskeleton, nucleus and on the cell surface where is transported in response to specific stimuli by unconventional mechanisms. Upregulation of RHAMM is observed during tissue remodeling (*e.g.* after injury or during tumorigenesis) and affects different cell functions as motility, migration, invasion and ECM remodeling.[41-45] Unlike CD44, RHAMM has no HA-binding module domain. Instead, it uses a BX_7B motif (B is either Lys or Arg and X_7 contains no acidic residues) on its COOH terminus to bind HA.[46, 47]

There is a significant body of evidence that supports the formation of a triple complex between CD44, RHAMM and HA on the cell surface during tumorigenesis. In this complex, the role of RHAMM is to enhance the CD44 surface localization, stabilize the CD44-HA interaction and thus, contribute to the activation of Erk1/2 signaling.[42-44] Besides this role, the presence of RHAMM in different cellular compartments and at the cell surface suggests that it might contribute to the signal transmission across the cell membrane.[38] However, the association dynamics between CD44 and RHAMM upon HA binding and the feedback responses are not completely understood. In this study we used Förster resonance energy transfer (FRET) and co-immunoprecipitation to follow the dynamics in CD44 and RHAMM expression and clustering in response to exogenously supplemented HA (Fig. 1).

1. Materials and Methods

2.1. Materials. Sodium hyaluronate (HA, average molecular weight of 4.8 kDa, polydispersity of 1.181) was obtained from Lifecore (USA). The antibodies used in this study were: human anti-CD44 PE (BD Pharmingen), RHAMM (H-8) (Santa Cruz Biotechnology), anti-CD168 antibody [EPR4055] (Abcam), anti-CD44 antibody [KM201] (abcam) monoclonal antibody to CD44 – Ascites (Acris), monoclonal antibody phospho-p44/42 MAPK (Erk1/2) (Thr202/Tyr204) (Cell Signaling), mouse IgG1, clone MOPC-21 (StemCell Technologies), AlexaFluor® 594 donkey anti-mouse IgG1 (H+L) and AlexaFluor® 488 donkey anti-rabbit IgG (H+L) (Molecular Probes).

2.2. Cell cultures. We studied MDA-MB-231 and Sk-Br-3 breast cancer cell lines. Cells were seeded on tissue culture polystyrene (TCPS) at 37 °C in Dulbecco Modified Eagle Medium (DMEM) high glucose with phenol red (Sigma-Aldrich) supplemented with 3.7 mg/mL sodium bicarbonate

(Sigma-Aldrich), 10 % fetal bovine serum (FBS, Invitrogen) and 1 % antibiotic/antimycotic (Invitrogen). Upon confluence, the cells were detached with TrypLE Express™ (Invitrogen) and used in the following experiments at cell density of $5x10^5$ cells/mL.

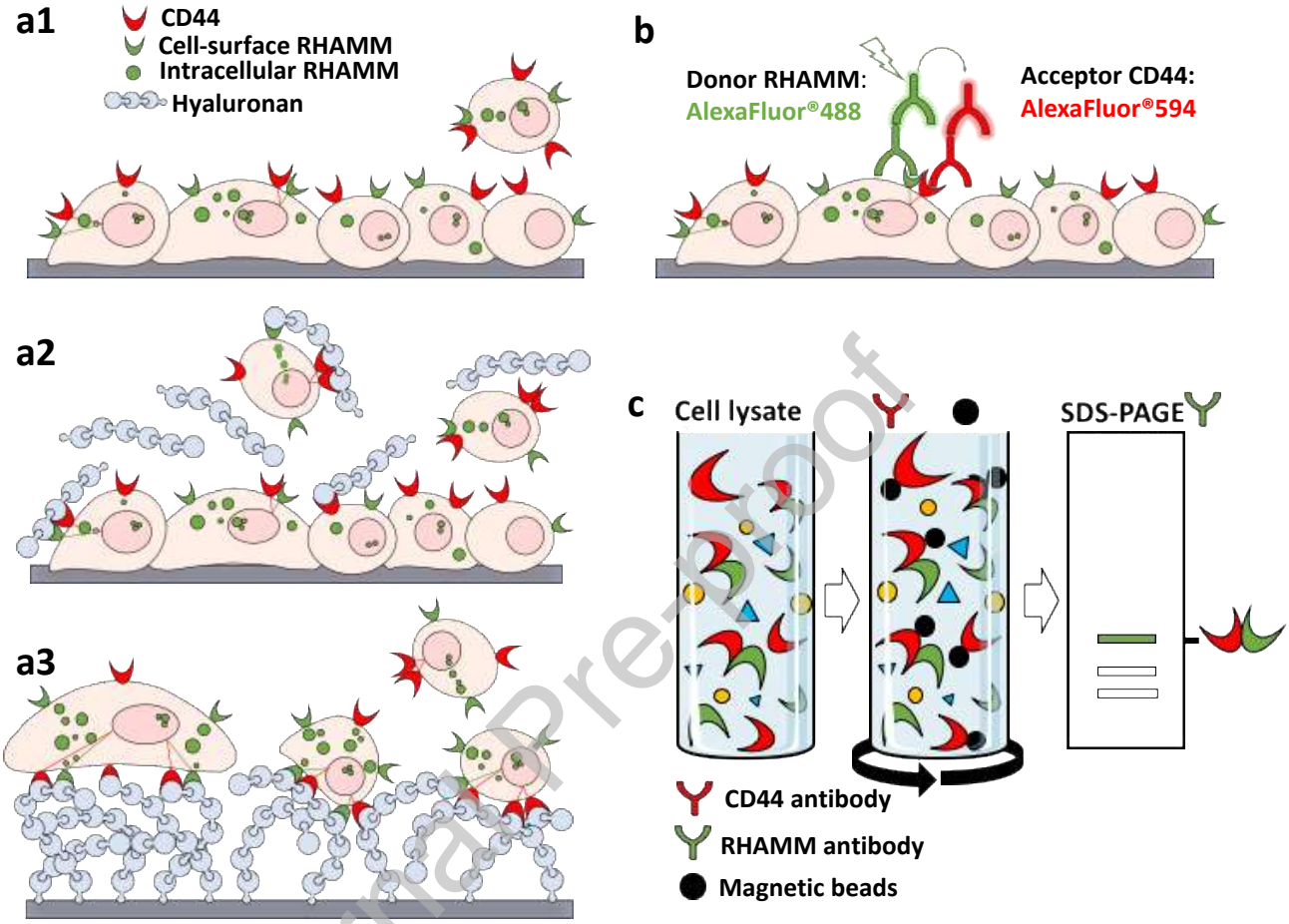


Figure 1. Schematic presentation of the experimental setup. (a) Cells culture conditions used: **(a1)** cells cultured on tissue culture polystyrene (TCPS) in the absence of exogenous hyaluronan (controls); **(a2)** cultures supplemented with hyaluronan dissolved in the media; and **(a3)** cells seeded on substrates with end-on immobilized hyaluronan. **(b)** Determination of the proximity of CD44 and RHAMM using immunocytochemistry combined with Förster resonance energy transfer (FRET). **(c)** Characterization of RHAMM/CD44 co-localization by co-immunoprecipitation.

2.3. Hyaluronan-supplemented cell cultures. Cells were seeded on TCPS coverslips (Fig. 1a) and after 24 h were supplemented with 0.5 mg/mL of HA (soluble HA, Fig. 1b) and kept for additional 24 h in contact with the HA. The substrates with immobilized HA were obtained by overnight incubation of a gold-coated glass with end-on modified HA (details are provided in the Suppl Info).

Journal Pre-proof

Cells were directly seeded on these substrates for 24 h (Fig. 1c). At the end of each experiment, cells were washed with PBS and fixed with 10 % formalin (Thermo Scientific) for further processing. Cells seeded on TCPS coverslips for 24 h were used as controls.

2.4. Pericellular hyaluronan coat. Cells were cultured on TCPS as described above. After 24 h and 48 h of culture, cells were fixed with 10 % formalin (1 h, 4 °C). Samples were stained with biotinylated HA binding protein (HAbp) from bovine nasal cartilage (1 μg/mL, 1 h at room temperature, Millipore) followed by incubation with streptavidin-AlexaFluor® 488 conjugate (1 μg/mL, 10 minutes room temperature, Molecular Probes). Images were acquired using an Inverted Confocal Microscope (TCS SP8, Leica).

2.5. Expression of hyaluronan receptors RHAMM and CD44 at the cell surface (flow cytometry). Cells were cultured as described above. Upon confluence, they were detached with 4 mM ethylenediaminetetraacetic acid (EDTA) in phosphate buffered saline (PBS pH 8, Sigma-Aldrich) and membrane expression of CD44 and RHAMM was characterized. Direct labelling of cells with anti-human CD44-PE was performed at room temperature for 20 min (0.2 μg/mL of the antibody for $5x10^5$ cells in 100 μL PBS). RHAMM tagging was performed in two steps: cells were incubated with mouse anti-human RHAMM (H-8) at 4 °C for 40 min (0.3 μg/mL of the antibody for $5x10^5$ cells in 100 μL PBS), followed by washing step and incubation with 0.1 μg/mL of secondary antibody AlexaFluor® 488 donkey anti-mouse IgG (H+L) (100 μL PBS, 40 min, 4 °C). Cells were fixed with 1 % formalin/PBS (1 h at 4 °C). Fluorescence was measured in BD FACSCaliburflow cytometer (BD Biosciences) and data was analyzed with Flowing software.

2.6. Total expression of RHAMM and CD44 (immunocytochemistry). Cells were fixed with 10 % formalin and permeabilized with 0.2 % of triton-X-100/PBS (15 min, room temperature). Unspecific interactions were blocked with 3% BSA/PBS (1 h, room temperature). Incubation with primary antibody was performed in 1% BSA/PBS for 1 h at room temperature. Anti-CD168 antibody (dilution 1:300) was used for RHAMM and CD44 were tagged with monoclonal antibody to CD44 (dilution 1:400). IgG1 (dilution 1:400) was used as isotype control. After thorough washing with PBS (3x 5 min), a secondary antibody (AlexaFluor® 488 (dilution 1:600) for RHAMM and AlexaFluor® 594 (dilution 1:600) for CD44 was added in 1% BSA/PBS (1 h at room temperature), together with DAPI (1 μg/mL) for nucleus counterstaining. Microscope slides were prepared with VectaShield mounting

medium (Vector Laboratories, USA). Images were acquired by an Inverted Confocal Microscope (TCS SP8, Leica). At least 30 cells were analyzed per condition.

2.7. Förster resonance energy transfer (FRET) measurements. FRET-based immunocytochemistry was performed with AlexaFluor® 488 (RHAMM, dilution 1:600) and AlexaFluor® 594 (CD44, dilution 1:600) as donor/acceptor (RHAMM/CD44) FRET pair. For double immunostaining, a blocking step with 3% BSA/PBS (overnight, 4 °C) was performed between procedures. FRET images were acquired on a confocal laser scanning microscope (TCS SP8, Leica) using a 63x immersion objective. For sensitized fluorescence emission measurement, images were acquired sequentially through DAPI, AlexaFluor® 488, FRET and AlexaFluor® 594. The microscopy sets used were: DAPI λ_{ex} = 405 nm and λ_{em} = 415 – 485 nm; AlexaFluor® 488 λ_{ex} = 488 nm and λ_{em} = 494 – 576 nm; AlexaFluor® 594 λ_{ex} = 461 nm and λ_{em} = 587 – 709 nm; and FRET λ_{ex} = 488 nm and λ_{em} = 587 – 709 nm.

ImageJ was used to determine the mean grey intensity within cells pixel-by-pixel. Images were saved in TIFF format (LAS X, Leica) and processed by ImageJ 1.52p. Images were imported in a virtual stack and converted to 8-bit images. After sum projection of Z stacks, the threshold was determined for each cell using *Moments Method* and the grey value was measured for the studied conditions. Corrected FRET was determined by subtracting the spectral bleed-through of AlexaFluor® 488 signal to AlexaFluor® 594 channel. Bleed-through of AlexaFluor® 488 into AlexaFluor® 594 channel was determined at each condition and cell line used. Corrected FRET ($FRET_{corr}$) signal was calculated by equation 1 (eq. 1):

$$FRET_{corr} = FRET_{total} - (a\ x\ donor) \qquad \text{(eq. 1)}$$

where $FRET_{total}$ is the total FRET signal measured, α *is* the fraction of bleed-through of AlexaFluor® 488 to acceptor channel (Table S1) and the *donor* is the Alexa Fluor® 488 signal measured. At least 30 cells were analyzed per condition.

2.8. Acceptor photobleaching-based FRET measurements. To determine FRET efficiency (*E*), photobleaching assays were performed. The photobleached area was manually selected and defined as a region of interest (ROI). Photobleaching experiments were performed using a confocal laser scanning microscope (TCS SP8, Leica). A pulse of high intensity laser (561 nm) was applied for 30 sec to locally bleach the signal of the acceptor (AlexaFluor® 594) in the ROI. Pre-bleaching and

post-bleaching images were acquired (AlexaFluor® 488 channel) as described above for FRET imaging. We verified the emission of the acceptor (CD44-tagged cells) at the donor excitation wavelength and determined negligible crosstalk at all studied conditions. The FRET efficiency (*E*) was calculated by eq. 2:

$$E = \frac{(F_{pos} - F_{pre})}{F_{pos}} \times 100 \qquad \text{(eq. 2)}$$

where F_{pre} and F_{pos} are the fluorescence intensity of the donor (Alexa Fluor® 488 channel) before and after acceptor photobleaching respectively.[48] At least 3 assays were made per condition.

2.9. Co-immunoprecipitation assay. All materials and reagents were ice-cooled; cells and cell lysates were kept over ice. Co-immunoprecipitation was performed following a previously described protocol.[42] Briefly, cells were seeded at a density of $4x10^4$ cells/cm^2 and maintained in culture for 24 h (control) or exposed to exogenous HA (soluble or immobilized) for 24 h as described in part 2.3. Cells were washed with PBS and lysed with freshly supplemented RIPA buffer (25 mM Tris-HCl, pH 7.2, 0.1 % SDS, 1 % Triton-X-100, 1 % sodium deoxycholate, 150 mM NaCl, 1 mM EDTA and 50 nM HEPES pH 7.3) containing the proteases inhibitor cocktail (1:50) (Sigma-Aldrich), phenylmethylsulphonyl fluoride (PMSF, 2 mM), 3,4-dichloroisocoumarin (200 mM), sodium orthovanadate (1 mM), and sodium fluoride (NaF, 1 mM). The obtained cell lysate was passed 10x through a 1 mL syringe equipped with a 27 G needle, cooled down (20 min on ice) and centrifuged (13 000 *g*, 20 min, 4 °C). Protein concentration in the supernatant was determined with Micro BCA™ Protein assay kit (ThermoFisher Scientific). Co-immunoprecipitation was performed using 200 μg of protein from each cell lysate. We performed two sets of experiments: in the first one, the lysates were mixed with primary antibody for RHAMM precipitation, namely anti-CD168 (6 μL) while in the second one a monoclonal antibody to CD44 (6 μL) was used to precipitate CD44. Immunoprecipitation with IgG1 (6 μL) was used as a control. Incubation of the lysate with the respective antibodies was performed at 4 °C for 12 h in a tube rotator. Next, 12 μL of a suspension of functionalized magnetic beads (Protein G Mag Sepharose™, GE Healthcare) was added and the samples were mixed for 6 h at 4 °C. The beads were separated from the supernatant with a magnetic rack and washed 3x with 0.5 % Triton-X-10/PBS. Bound proteins were released from the beads by boiling the samples in 25 μL of 1X Laemmli buffer for 10 min. Recovered protein from each cell lysate was loaded and separated by electrophoresis on a 12 % SDS-PAGE together with

PageRuler™ Plus pre-stained protein ladder (Thermo Scientific). Proteins were then transferred to Amersham™ Protan® blotting membranes (Merk) with Bjerrum Schafer-Nielsen Buffer (48 mM Tris-HCl, 98 mM glycine, 20 % methanol and 1.3 mM SDS) by the semi-dry method in a Pierce Power Station (Thermo Scientific). Protein binding sites on the membrane were blocked by incubation with 5 % skimmed milk, 1 % BSA and 0.5 % Tween-20/TBS-T (50 mM Tris base pH 7.6, 150 mM NaCl, 0.1 % Tween-20) for 30 min at room temperature. The membranes were incubated with primary antibodies in 1% BSA/TBS-T overnight at 4 °C: anti-CD168 (diluted 1:4000) was used in the case of immunoprecipitated CD44 and monoclonal antibody to CD44 (diluted 1:10000) was used for immunoprecipitated RHAMM. The membranes were washed 3x 15 min with TBS-T. Immunodetection was performed using anti-rabbit or anti-mouse IRDye (diluted 1:10000, Li-Cor) in 1 % BSA/TBST for 1 h at room temperature followed by washing with TBS-T (3x 5 min) and TBS. Blotting was visualized using Odyssey® Fc Imaging System (Li-Cor).

2.10. Erk1/2 activation. Erk1/2 activation was evaluated through immunocytochemistry. Immunocytochemistry was performed as described above using monoclonal antibody phospho-p44/42 MAPK (Erk1/2) (dilution 1:200) and secondary antibody anti-rabbit AlexaFluor® 488 (dilution 1:600). Images were acquired in Inverted Confocal Microscope (TCS SP8, Leica) and at least 30 cells were used for image analysis.

2.11. Statistical analysis. All experiments were repeated at least two times and at least three images were acquired with the same parameters. The results are presented as mean ± standard deviation. Statistical differences among data with homogeneous variance were assessed by analysis of variance (ANOVA), followed by Tuckey posthoc test. Data that did not follow normal distribution were analyzed with Kruskal-Wallis test. All tests were performed with a 95% significance.

2. Results and Discussion

3.1. Characterization of selected breast cancer cells. We selected two breast cancer cell lines, MDA-MB-231 and Sk-Br-3, based on previous reports describing different invasive properties and expression of HA receptors for these cells.[35, 42, 49-52] MDA-MB-231 cells are invasive and have a motile phenotype, while Sk-Br-3 cells are described as non-invasive.[51, 52] We characterized these

cell lines in terms of HA deposition in the pericellular space and surface expression of main HA receptors (Fig. 2 and Table S2) and indeed, observed different profiles.

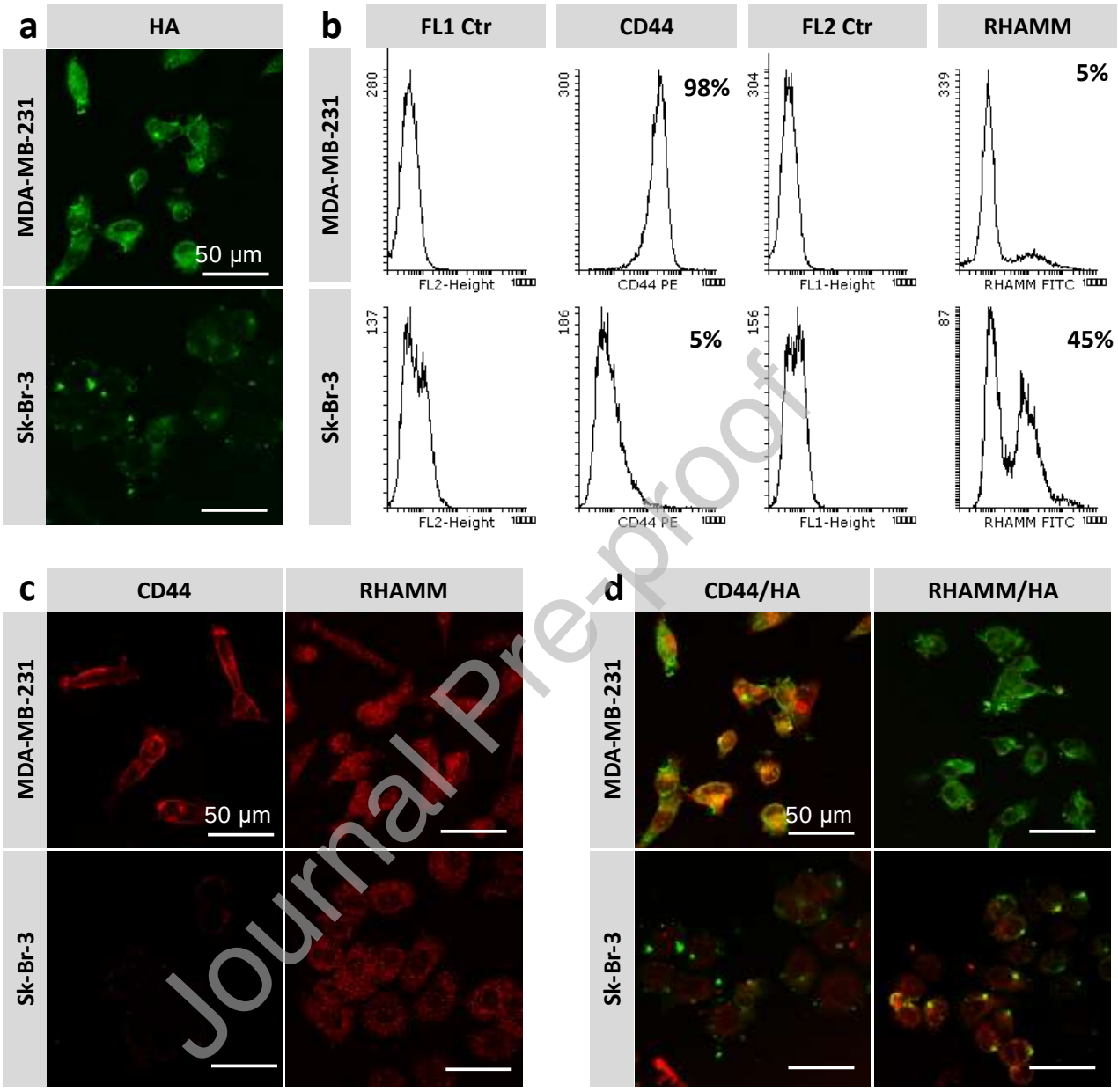


Figure 2. Characterization of breast cancer cell lines MDA-MB-231 and Sk-Br-3: **(a)** Confocal microscopy images showing the endogenous hyaluronan secreted by MDA-MB-231 and Sk-Br-3; **(b)** Flow cytometry analysis showing unstained (FL1 and FL2 control) and immuno-tagged CD44 and RHAMM at the surface of the studied cell lines; **(c)** Total expression of CD44 and RHAMM visualized by confocal microscopy of immunostained and permeabilized cells; **(d)** Confocal microscopy images showing secreted hyaluronan (green) and its receptors (red) CD44 and RHAMM. Cells were cultured

Journal Pre-proof

on TCPS for 24 h. Supplementary information about the flow cytometry analysis of permeabilized and non-permeabilized cells are reported in Fig. S4 and Table S2.

MDA-MB-231 cells presented HA-rich coat while less HA is visible around Sk-Br-3 and this difference increases with the culture time (Fig. 2a and Fig. S3). These results suggest that MDA-MB-231 and Sk-Br-3 have different HA metabolism. The HA recognition apparatus is also distinct: flow cytometry data of non-permeabilized MDA-MB-231 cells showed that they are CD44 positive and contain a small population (about 5%) of RHAMM positive cells (Fig. 2b, Table S2). On the contrary, a bigger population of RHAMM positive cells and few cells that express CD44 on the surface were presented in the Sk-Br-3 cells culture. Total expression (membrane and cytoplasmic) of CD44 followed the same trend (Figs. 2c and S4): higher CD44 expression is visible for MDA-MB-231 whereas Sk-Br-3 cells have a weak CD44 signal. The total expression of RHAMM was similar for both cell lines. Localization of RHAMM and CD44 is critical for their function(s) and contribution to cancer cell aggressiveness.[18, 36, 39] CD44 is co-localized with the endogenous HA in MDA-MB-231 cells but not in SkBr-3 cells where mainly cytoplasmic CD44 is expressed (Figs. 2d and S4). RHAMM is mostly located in the cytoplasm for both cell lines although higher surface expression was observed in Sk-Br-3 cells as compared with MDA-MB-231 cells. Intracellular RHAMM affects cytoskeleton dynamics, cell proliferation and genomic instability, contributing to tumor cell susceptibility and aggressiveness.[36, 38, 44, 53-55] Cell-surface RHAMM, on the other hand, can bind to HA and associate with other proteins, *e.g.* CD44. Mechanistically, it has similar functions to CD44, *i.e.* increases invasiveness in breast cancer.[39, 56]

3.2 HA induces feedback on CD44 and RHAMM expression. The effect of HA on cancer cells is mainly studied upon supplementation of culture media with soluble HA or its oligomers (Fig. 1a2). Such presentation differs from the one observed in the ECM and pericellular space where HA spatial freedom is confined by its interactions with other biomolecules resulting in the formation of concentration gradients and spatial definition of its binding sites.[1, 20] Thus, in addition to supplementation with soluble HA, we also studied cultures on substrates with end-on immobilized HA (Figs. S1 and S2). Such immobilization does not affect HA structure and does not compromise its bioactivity but allows limited HA spatial freedom and increased local concentration, *i.e.* it mimics the HA-rich pericellular coats.[20, 22, 57, 58]

Journal Pre-proof

Soluble HA did not induce any significant changes in the studied cultures (Fig. 3). On the other hand, immobilized HA affected both cell lines. RHAMM expression was significantly increased in MDA-MB-231 and SkBr-3 cells (Fig. 3c, d). This result is in agreement with previous studies showing that HA–RHAMM interaction can activate a signal transduction pathway resulting in both mRNA production and protein overexpression, and RHAMM mobilization to the cell surface.[38] RHAMM overexpression was concomitant with decreased CD44 expression in MDA-MB-231 cells, *i.e.* CD44 positive cells (Fig. 3a, 3c). Such compensatory effect between CD44 and RHAMM has been previously described and it is consistent with the concept of molecular redundancy.[41, 56]

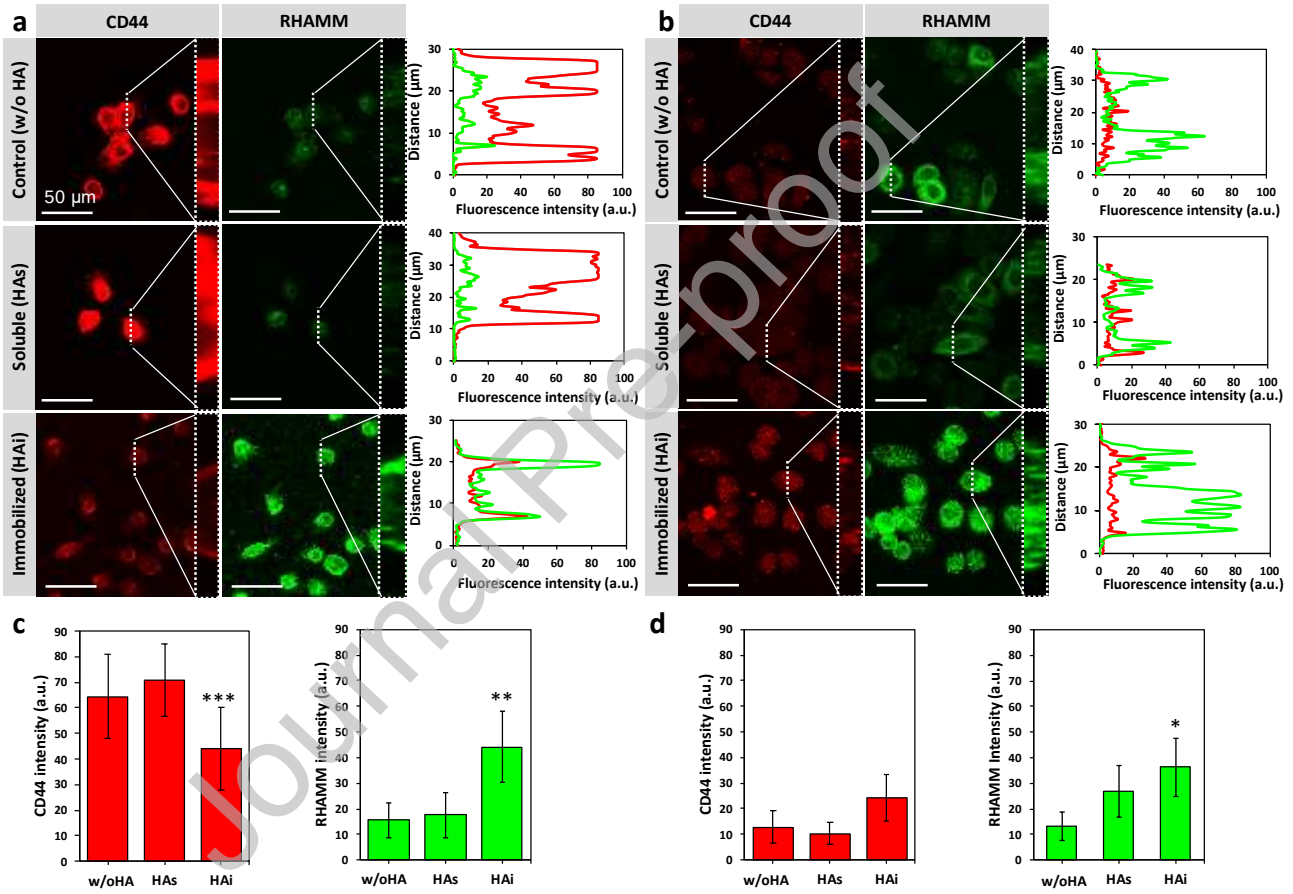


Figure 3. Expression of CD44 (red) and RHAMM (green) by **(a, c)** MDA-MB-231 and **(b, d)** Sk-Br-3 cells cultured at the studied conditions. Maximum projections (z-stacks) and orthogonal YZ (lateral inserts) confocal microscopy images of **(a)** MDA-MB-231 and **(b)** Sk-Br-3 cultures. The images show the total expression of CD44 (red) and RHAMM (green) and the respective distribution of these proteins across the cells (lateral images inserts and graphs). Non-immune IgG1 was used as an isotype control (Fig. S5). Average fluorescence intensity showing the relative total expression of

CD44 and RHAMM in **(c)** MDA-MB-231 and **(d)** Sk-Br-3 cells cultured at the studied conditions. Statistical differences between HA cultures and control: *$p \leq 0.05$; **$p < 0.005$ and ***$p < 0.001$.

The recognition and binding to HA *via* CD44 activate different signaling cascades including HA endocytosis.[3, 59] When MDA-MB-231 cells are cultured on immobilized HA, CD44 recognizes and binds HA but its endocytosis is hampered.[59] As a result, the expression of CD44 is reduced (as it is "blocked") and RHAMM is overexpressed to compensate it. The magnitude of these changes is proportional to the initial level of CD44 expression, *i.e.* more dramatic changes are observed for cells with higher expression of CD44. Immunostaining showed that the overexpressed RHAMM is localized also in the cytoplasm (Fig. 3a) suggesting its involvement in the intracellular signaling upon HA binding. In Sk-Br-3 cells both RHAMM and CD44 are expressed (Fig. 2b) but the competition between them for HA binding is different as more RHAMM is expressed on the cell surface. Upon exposure to immobilized HA, these cells overexpressed both receptors but the induced changes in RHAMM expression are greater as compared with CD44 (Fig. 3d).

3.3 Immobilized HA induces CD44/RHAMM complexation. We used FRET to study possible co-localization of CD44 and RHAMM (Fig. 1b) upon HA exposure.[60] Herein, we took the advantages of the secondary antibodies used for detection of RHAMM (AlexaFluor® 488, donor) and CD44 (AlexaFluor® 594, acceptor). These secondary antibodies were specifically chosen to maximize the energy transfer: there is a 96% overlapping between AlexaFluor® 594 excitation spectrum with the emission spectrum of AlexaFluor® 488 and only 10% of the emission spectrum of AlexaFluor® 488 matches with the emission spectra of AlexaFluor® 594, thus avoiding signal bleed through (Fig. S7). While the use of the antibodies for FRET measurements can compromise the resolution, this approach can be very useful in a clinical scenario and as a fast pre-screening method. Moreover, FRET is more reliable than the conventional signal overlap of confocal micrographs/channels often applied to show co-localization of immunolabelled proteins.[61, 62]

We detected FRET for both studied cell lines, but the signal had different intensity (Fig. 4, controls): most intense signal is visible for the invasive MDA-MB-231 cell line (Fig. 4c *vs* Fig 4d). Of note, FRET was detected both intracellular and on the surface of these cells, indicating co-localization of RHAMM and CD44 at these locations. The intracellular signal, however, was weaker showing predominant co-localization of RHAMM and CD44 at the cell surface. The low intensity of FRET signal of Sk-Br-3 cells (Fig. 4b, d, controls) suggests that RHAMM on the cell surface is not co-

localized with CD44. Previous studies have shown that once translocated to the cell surface RHAMM can complex not only with CD44 but also with other receptors such as PDGFR, TGFβ Receptor-1, bFGFR and RON among others.[41, 43, 44, 63-68]

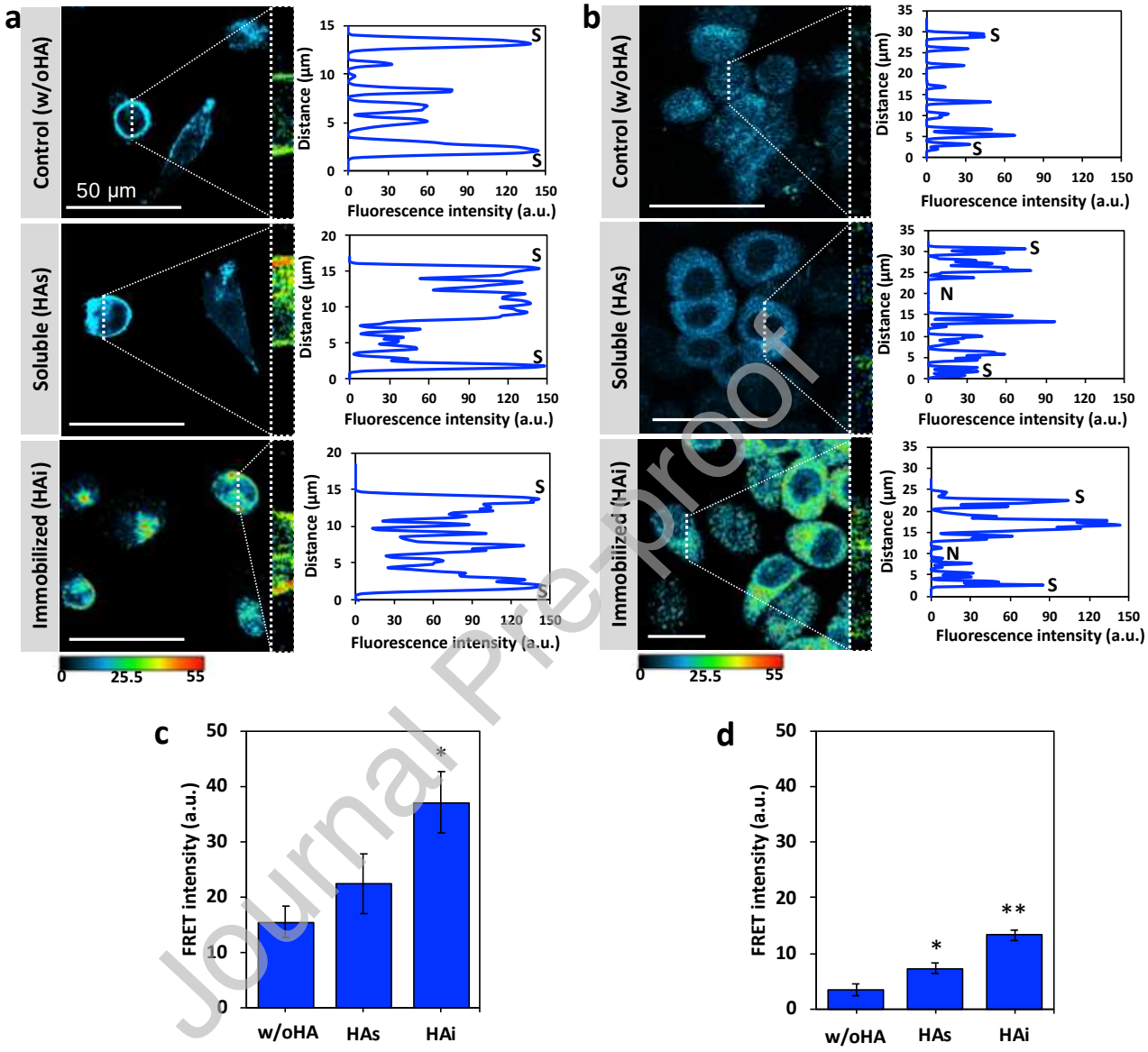


Figure 4. FRET-based immunocytochemistry of **(a, c)** MDA-MB-231 and **(b, d)** Sk-Br-3 cultured in the absence of exogenous HA (controls, w/oHA) or conditioned with soluble HA (HAs) or immobilized HA (HAi). **(a, b)** The images show maximum and orthogonal (lateral inserts) projections obtained by confocal microscopy together with the respective distribution of signal intensity across the cells (S: surface, N: nucleus). FRET signals were acquired at 594 nm channel after excitation at 488 nm in both RHAMM and CD44 immunostained cells. **(c, d)** Graphical presentation of average FRET intensity after correction for bleed-through for **(c)** MDA-MB-231 and **(d)** Sk-Br-3 cells. Controls

showing unspecific binding of secondary antibodies are presented in Fig. S5. Lower resolution images and bleed-through signals are shown in Fig. S7. Statistical differences between HA supplemented cultures and control: *$p \leq 0.05$ and **$p < 0.005$.

The obtained data indicated that the main HA receptors in the studied cell lines have not only different expression but might be also engaged in different cell-surface interactions and thus, anticipated different cellular responses upon HA supplementation. FRET signal did not show any substantial changes in RHAMM/CD44 complexes upon supplementation of MDA-MB-231 with soluble HA, while an increased co-localization of these receptors was observed for Sk-Br-3 cells at these conditions. On the other hand, a significant increase of the FRET signal intensity was obtained for cells seeded on immobilized HA (Fig. 4). This change suggests that the interaction with immobilized HA results in RHAMM overexpression and co-localization with CD44.

FRET/RHAMM signal ratio is proportional to FRET efficiency, which depends on receptors proximity (Fig. S8).[33] The FRET/RHAMM signal ratio was constant and close to 1 for MDA-MB-231 at all studied conditions. In Sk-Br-3 cells, this ratio was 0.2 when cells were seeded on TCPS or supplemented with soluble HA. These results show close localization of RHAMM and CD44 in MDA-MB-231 but not in Sk-Br-3 cells and indicate that CD44 and RHAMM can participate in different protein complexes in the studied cell lines. However, when Sk-Br-3 cells were cultured on immobilized HA, FRET/RHAMM signal ratio increased significantly to about 0.8 evidencing possible complexation between RHAMM and CD44 at these conditions. Acceptor photobleaching at a selected region of interest (ROI) was performed for cells seeded over immobilized HA to determine FRET efficiency. Photobleaching of CD44 (acceptor) leads to a decrease of the FRET signal and increase of the average intensity of RHAMM (donor) signal (Figs. 5 and S9). The average energy transfer efficiency for cells seeded on immobilized HA was calculated and we obtained FRET efficiency of 28.49 ± 8.2 % for MDA-MB-231 cells and 3.75 ± 3.2 % for Sk-Br-3 cells. These results suggest co-localization of CD44 and RHAMM in MDA-MB-231 cells seeded on immobilized HA but are not conclusive for Sk-Br-3 cells. We therefore studied the possible complexation of CD44 and RHAMM by co-immunoprecipitation (Fig. 6).

Journal Pre-proof

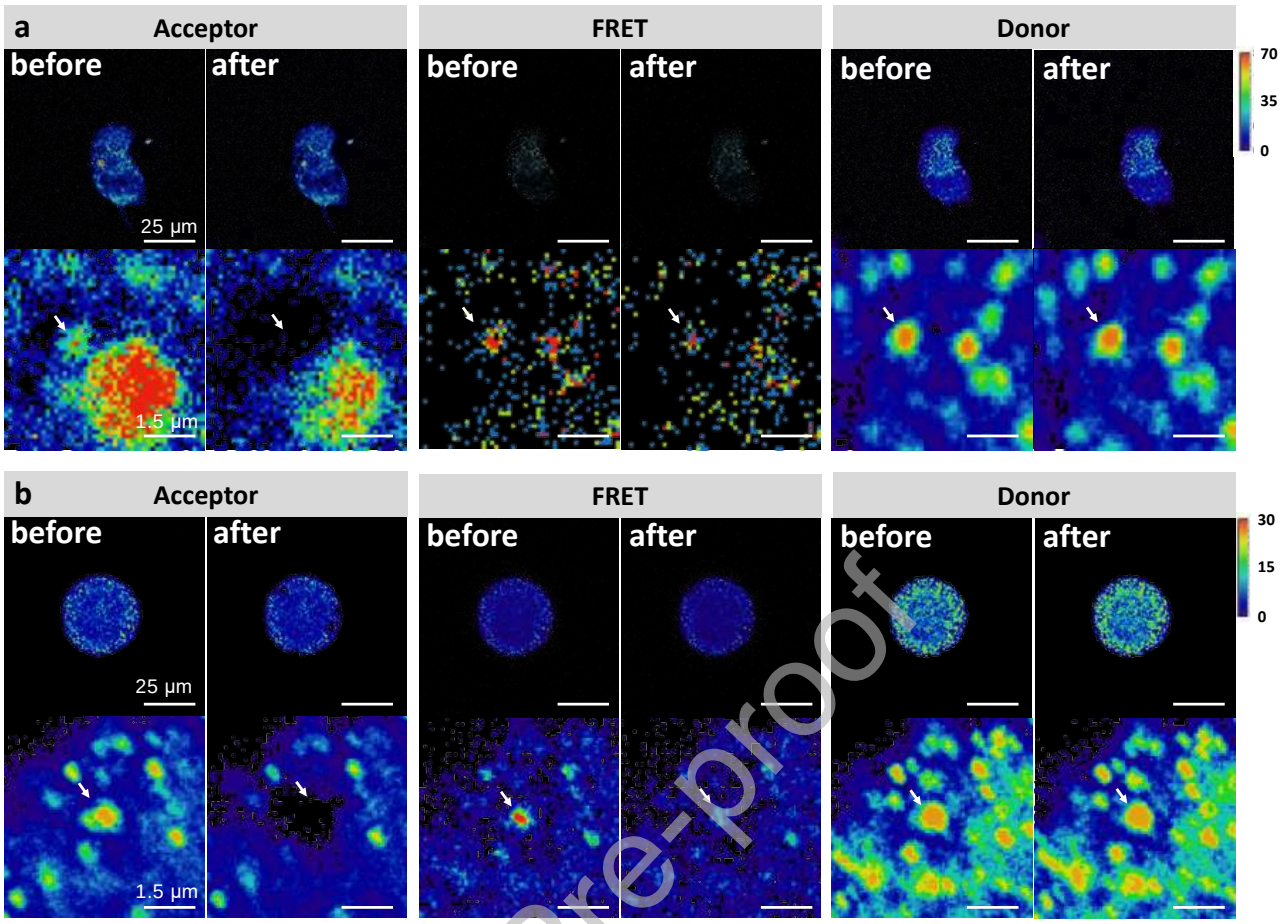


Figure 5. Representative photobleaching FRET data showing RHAMM/CD44 complexation in **(a)** MDA-MB-231 and **(b)** Sk-Br-3 cells. Local photobleaching of the acceptor results in FRET signal decreasing and donor signal increasing (indicated with arrows).

In control samples (without exogenous HA supplementation), anti-CD168 antibodies co-immunoprecipitated two CD44 isoforms in the case of MDA-MB-231 cells (50 and 77 kDa, Fig. 6a) and three CD44 isoforms in Sk-Br-3 cells (50, 70 and 85 kDa, Fig. 6b). These sizes correspond to the standard CD44 (85 kDa) and to truncated forms of CD44.[42, 69] In reciprocal immunoprecipitation assay (anti-CD44 antibodies co-immunoprecipitated RHAMM; Fig. 6c, d) we detected two RHAMM isoforms (43 and 70 kDa).[42, 70] Supplementation with HA induced increase of RHAMM/CD44 co-localization in MDA-MB-231 cells that was more pronounced (2.5-fold) in the case of immobilized HA (Fig. 4c). The trend was the same for Sk-Br-3 cells (RHAMM is the main surface HA-receptor) but the magnitude was bigger: we observed 6-fold higher co-localization for cells seeded on immobilized HA when compared to the control (Fig. 6d).

Journal Pre-proof

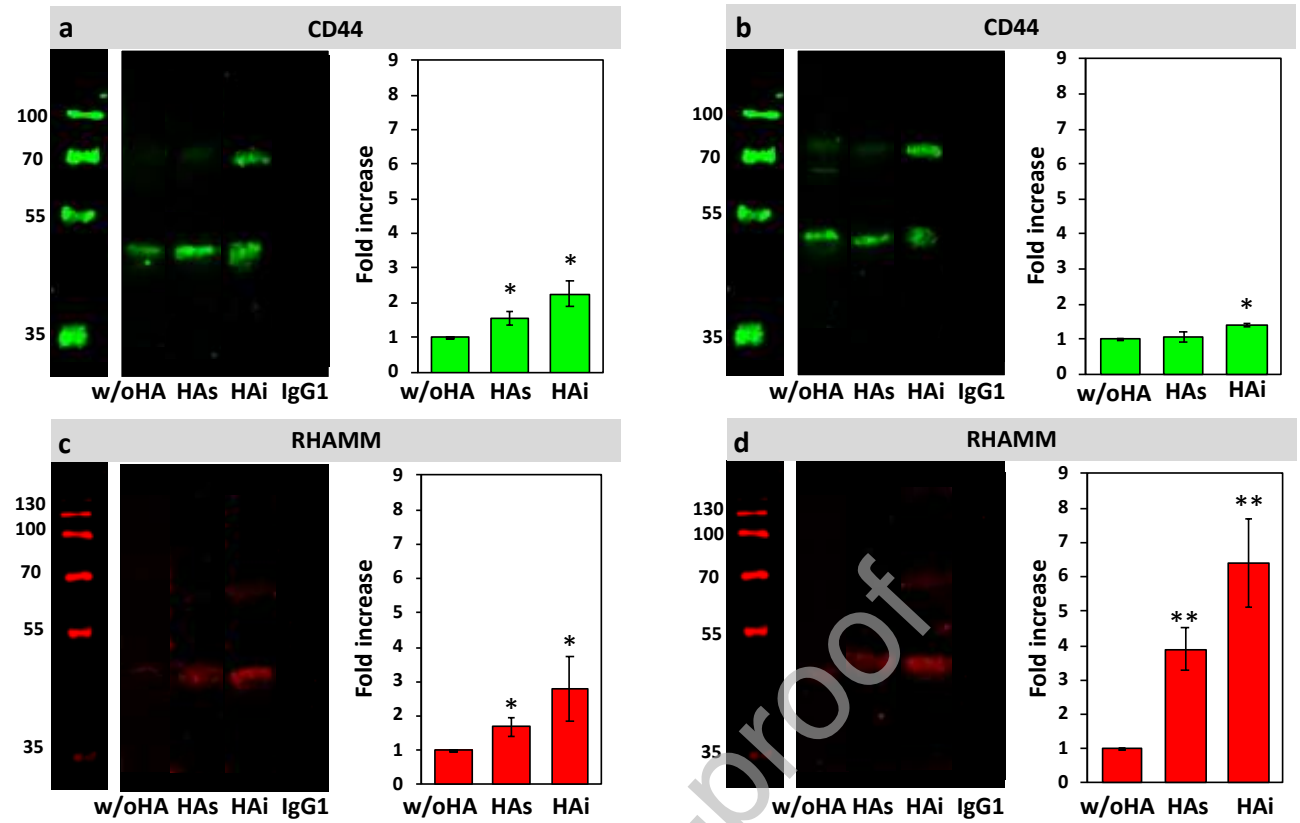


Figure 6. Western blot of (**a, b**) RHAMM immunoprecipiated with CD44 detection (green) and (**c, d**) CD44 immunoprecipitate with RHAMM detection (red) together with the respective densitometry quantification (fold increase as compared to the control without HA) for (**a, c**) MDA-MB-231 and (**b, d**) Sk-Br-3 cells cultured at the studied conditions. Non-immune IgG1 was used for immunoprecipitation control. HAs: soluble hyaluronate; HAi: immobilized hyaluronate.

Western blot analysis of non-immunoprecipitated proteins showed that not all CD44 co-localizes with RHAMM in MDA-MB-231 cells at the studied conditions (Fig. S10a, green). This result is expected keeping in mind the high expression of CD44 by these cells. On the other hand, non-immunoprecipitated CD44 was not detected for Sk-Br-3 cells, *i.e.* for these cells all CD44 is engaged with RHAMM (Fig. S10c). The results for non-immunoprecipitated RHAMM confirmed that HA supplementation (either soluble or immobilized) promotes CD44/RHAMM co-localization (Fig. S10b, d). Of note, in the case of Sk-Br-3 cells cultured on immobilized HA, we did not observe any non-immunoprecipitated CD44 and RHAMM indicating an optimal co-localization of the two proteins at these conditions. Altogether, these results confirmed FRET data and showed that RHAMM/CD44 co-localization depends on HA presentation and on the expressed cell surface receptor(s).

Journal Pre-proof

3.4. Erk1/2 activation. Interaction of HA with CD44 and RHAMM can activate different signaling pathways towards cell survival, proliferation and migration/motility. Among these, Erk1/2 is known to be HA-dependent and to regulate cell migration in invasive breast cancers.[42] We evaluated the activation of Erk1/2 in the studied cell lines by immunocytochemistry (Fig. 7). We found that MDA-MB-231 and Sk-Br-3 cells have similar basal levels of active Erk1/2. A slight increase of Erk1/2 activation was found in MDA-MB-231 cells seeded on immobilized HA while supplemented soluble HA did not affect this pathway. On the other hand, a significant increment of Erk1/2 activation was found for Sk-Br-3 cells at both studied conditions. These results show an effect of HA presentation beyond cell surface receptors co-localization. The increased RHAMM expression and co-localization were observed for the same conditions (immobilized HA for both cell lines and soluble HA for Sk-Br-3) and are indicative of RHAMM involvement in the regulation of Erk1/2 pathway and contribution to aggressive tumorigenic phenotype as previously proposed by other studies.[42, 71]

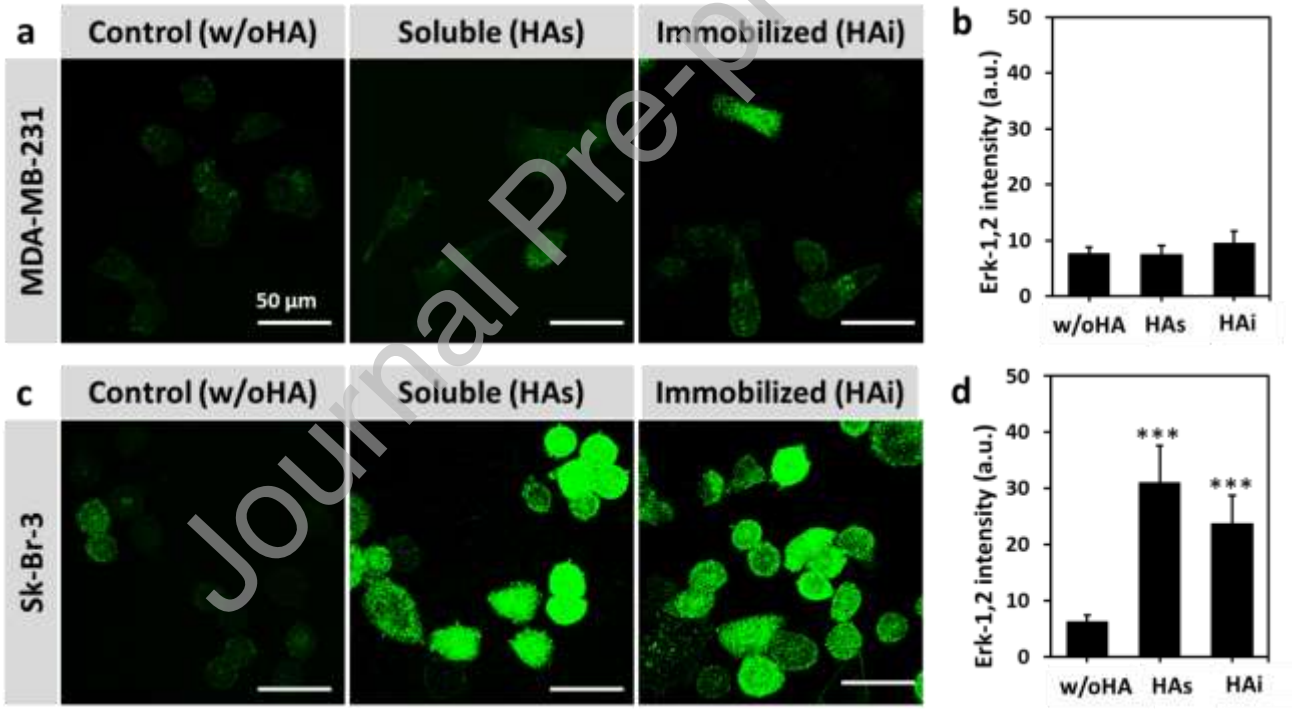


Figure 7. (a, c) Representative confocal images showing the activation of Erk-1,2 pathway (green) in **(a)** MDA-MB-231 and **(c)** Sk-Br-3 cells cultured in the absence (w/o HA) and presence of HA (soluble and immobilized); and **(b, d)** the respective graphical representation of active Erk-1,2 fluorescence intensity. Statistical differences between HA cultures and control are marked ***p< 0.001.

3. Conclusions

Our results suggested a link between HA presentation, CD44/RHAMM co-localization and cancer aggressiveness. Supplementation with exogenous, immobilized HA can enhance CD44/RHAMM co-localization and contribute towards an aggressive and invasive phenotype. In this process, RHAMM has manifold functions: to compensate CD44, to transduce the feedback response upon HA binding and to regulate signaling pathways.

Statement of Significance

The dynamics between CD44 and the receptor for hyaluronic acid-mediated motility (RHAMM) upon exposure to exogenously supplemented hyaluronan (soluble or immobilized) is described for invasive and non-invasive breast cancer cell lines. Co-localization of these two receptors is enhanced in the presence of immobilized hyaluronan. A link between the molecular recognition of hyaluronan and cell-specific feedback in the intracellular signaling cascade is proposed, in which RHAMM has a double function: to compensate CD44 and as a transducer of feedback response upon HA binding.

Declaration of interests

☒ The authors declare that they have no known competing financial interests or personal relationships that could have appeared to influence the work reported in this paper.

Journal Pre-proof

Acknowledgements

The authors thank the Portuguese Foundation for Science and Technology (FCT) (Grants SFRH/BD/114847/2016 and PTDC/NAN-MAT/28468/2017) and EU (Grant 668983-Forecast) for providing financial support to this project.

References

[1] B.P. Toole, Hyaluronan: From extracellular glue to pericellular cue, Nat Rev Cancer 4(7) (2004) 528-539.

[2] D. Vigetti, E. Karousou, M. Viola, S. Deleonibus, G. De Luca, A. Passi, Hyaluronan: Biosynthesis and signaling, Bba-Gen Subjects 1840(8) (2014) 2452-2459.

[3] W. Knudson, G. Chow, C.B. Knudson, CD44-mediated uptake and degradation of hyaluronan, Matrix Biology 21(1) (2002) 15-23.

[4] W. Knudson, E. Bartnik, C.B. Knudson, Assembly of Pericellular Matrices by Cos-7 Cells Transfected with Cd44 Lymphocyte-Homing Receptor Genes, Proceedings of the National Academy of Sciences of the United States of America 90(9) (1993) 4003-4007.

[5] S. Misra, L.M. Obeid, Y.A. Hannun, S. Minamisawa, F.G. Berger, R.R. Markwald, B.P. Toole, S. Ghatak, Hyaluronan constitutively regulates activation of COX-2-mediated cell survival activity in intestinal epithelial and colon carcinoma cells, J Biol Chem 283(21) (2008) 14335-14344.

[6] C.O. McAtee, J.J. Barycki, M.A. Simpson, Emerging Roles for Hyaluronidase in Cancer Metastasis and Therapy, in: M.A. Simpson, P. Heldin (Eds.), Hyaluronan Signaling and Turnover2014, pp. 1-34.

[7] P.H. Weigel, P.L. DeAngelis, Hyaluronan synthases: A decade-plus of novel glycosyltransferases, J Biol Chem 282(51) (2007) 36777-36781.

[8] A. Jacobson, J. Brinck, M.J. Briskin, A.P. Spicer, P. Heldin, Expression of human hyaluronan synthases in response to external stimuli, Biochem J 348 (2000) 29-35.

[9] R. Stern, Hyaluronidases in cancer biology, Seminars in Cancer Biology 18(4) (2008) 275-280.

[10] P. Heldin, K. Basu, B. Olofsson, H. Porsch, I. Kozlova, K. Kahata, Deregulation of hyaluronan synthesis, degradation and binding promotes breast cancer, J Biochem 154(5) (2013) 395-408.

[11] T. Chanmee, P. Ontong, N. Itano, Hyaluronan: A modulator of the tumor microenvironment, Cancer Lett 375(1) (2016) 20-30.

[12] K.L. Schwertfeger, M.K. Cowman, P.G. Telmer, E.A. Turley, J.B. McCarthy, Hyaluronan, inflammation, and breast cancer progression, Frontiers in Immunology 6 (2015) 1-12.

[13] P. Auvinen, R. Tammi, J. Parkkinen, M. Tammi, U. Agren, R. Johansson, P. Hirvikoski, M. Eskelinen, V.M. Kosma, Hyaluronan in peritumoral stroma and malignant cells associates with breast cancer spreading and predicts survival, American Journal of Pathology 156(2) (2000) 529-536.

[14] C. Tolg, J.B. McCarthy, A. Yazdani, E.A. Turley, Hyaluronan and RHAMM in Wound Repair and the "Cancerization" of Stromal Tissues, Biomed Research International (2014).

Journal Pre-proof

[15] H. Porsch, B. Bernert, M. Mehic, A.D. Theocharis, C.H. Heldin, P. Heldin, Efficient TGF beta-induced epithelial-mesenchymal transition depends on hyaluronan synthase HAS2, Oncogene 32(37) (2013) 4355-4365.

[16] P. Li, T.X. Xiang, H.Z. Li, Q.Q. Li, B. Yang, J. Huang, X. Zhang, Y. Shi, J.X. Tan, G.S. Ren, Hyaluronan synthase 2 overexpression is correlated with the tumorigenesis and metastasis of human breast cancer, Int J Clin Exp Patho 8(10) (2015) 12101-12114.

[17] N.F. Liu, F. Gao, Z.Q. Han, X.M. Xu, C.B. Underhill, L.R. Zhang, Hyaluronan synthase 3 overexpression promotes the growth of TSU prostate cancer cells, Cancer Research 61(13) (2001) 5207-5214.

[18] E.A. Turley, D.K. Wood, J.B. McCarthy, Carcinoma Cell Hyaluronan as a "Portable" Cancerized Prometastatic Microenvironment, Cancer Research 76(9) (2016) 2507-2512.

[19] K.A. Scheibner, M.A. Lutz, S. Boodoo, M.J. Fenton, J.D. Powell, M.R. Horton, Hyaluronan fragments act as an endogenous danger signal by engaging TLR2, J Immunol 177(2) (2006) 1272-1281.

[20] S. Amorim, D.S. da Costa, D. Freitas, C.A. Reis, R.L. Reis, I. Pashkuleva, R.A. Pires, Molecular weight of surface immobilized hyaluronic acid influences CD44-mediated binding of gastric cancer cells, Scientific Reports 8 (2018).

[21] C.X. Yang, M.L. Cao, H. Liu, Y.Q. He, J. Xu, Y. Du, Y.W. Liu, W.J. Wang, L. Cui, J.J. Hu, F. Gao, The High and Low Molecular Weight Forms of Hyaluronan Have Distinct Effects on CD44 Clustering, J Biol Chem 287(51) (2012) 43094-43107.

[22] P.M. Wolny, S. Banerji, C. Gounou, A.R. Brisson, A.J. Day, D.G. Jackson, R.P. Richter, Analysis of CD44-Hyaluronan Interactions in an Artificial Membrane System INSIGHTS INTO THE DISTINCT BINDING PROPERTIES OF HIGH AND LOW MOLECULAR WEIGHT HYALURONAN, J Biol Chem 285(39) (2010) 30170-30180.

[23] H. Ponta, L. Sherman, P.A. Herrlich, CD44: From adhesion molecules to signalling regulators, Nat Rev Mol Cell Bio 4(1) (2003) 33-45.

[24] S. Misra, V.C. Hascall, R.R. Markwald, S. Ghatak, Interactions between hyaluronan and its receptors (CD44, RHAMM) regulate the activities of inflammation and cancer, Frontiers in Immunology 6 (2015).

[25] A. Afify, P. Purnell, L. Nguyen, Role of CD44s and CD44v6 on human breast cancer cell adhesion, migration, and invasion, Exp Mol Pathol 86(2) (2009) 95-100.

[26] R.J. Peach, D. Hollenbaugh, I. Stamenkovic, A. Aruffo, Identification of Hyaluronic-Acid Binding-Sites in the Extracellular Domain of Cd44, Journal of Cell Biology 122(1) (1993) 257-264.

[27] S. Banerji, A.J. Day, J.D. Kahmann, D.G. Jackson, Characterization of a functional hyaluronan-binding domain from the human CD44 molecule expressed in Escherichia coli, Protein Expres Purif 14(3) (1998) 371-381.

[28] V. Orian-Rousseau, J. Sleeman, CD44 is a Multidomain Signaling Platform that Integrates Extracellular Matrix Cues with Growth Factor and Cytokine Signals, in: M.A. Simpson, P. Heldin (Eds.), Hyaluronan Signaling and Turnover2014, pp. 231-254.

[29] Y. Sohara, N. Ishiguro, K. Machida, H. Kurata, A.A. Thant, T. Senga, S. Matsuda, K. Kimata, H. Iwata, M. Hamaguchi, Hyaluronan activates cell motility of v-Src-transformed cells via Ras-mitogen-activated protein kinase and phosphoinositide 3-kinase-Akt in a tumor-specific manner, Mol. Biol. Cell 12(6) (2001) 1859-1868.

[30] Y. Fujita, M. Kitagawa, S. Nakamura, K. Azuma, G. Ishii, M. Higashi, H. Kishi, T. Hiwasa, K. Koda, N. Nakajima, K. Harigaya, CD44 signaling through focal adhesion kinase and its anti-apoptotic effect, FEBS Lett. 528(1-3) (2002) 101-108.

[31] L.Y.W. Bourguignon, E. Gilad, K. Peyrollier, Heregulin-mediated ErbB2-ERK signaling activates hyaluronan synthases leading to CD44-dependent ovarian tumor cell growth and migration, J Biol Chem 282(27) (2007) 19426-19441.

[32] J. Lesley, V.C. Hascall, M. Tammi, R. Hyman, Hyaluronan binding by cell surface CD44, J Biol Chem 275(35) (2000) 26967-26975.

[33] C. Yang, M. Cao, H. Liu, Y. He, J. Xu, Y. Du, Y. Liu, W. Wang, L. Cui, J. Hu, F. Gao, The High and Low Molecular Weight Forms of Hyaluronan Have Distinct Effects on CD44 Clustering, The Journal of Biological Chemistry 287(51) (2012) 43094-43107.

[34] L. Jiang, G.H. Liu, H.Y. Liu, J. Han, Z.B. Liu, H.C. Ma, Molecular weight impact on the mechanical forces between hyaluronan and its receptor, Carbohydrate Polymers 197 (2018) 326-336.

[35] C. Sheridan, H. Kishimoto, R.K. Fuchs, S. Mehrotra, P. Bhat-Nakshatri, C.H. Turner, R. Goulet, S. Badve, H. Nakshatri, CD44(+)/CD24(-) breast cancer cells exhibit enhanced invasive properties: an early step necessary for metastasis, Breast Cancer Research 8(5) (2006).

[36] P.G. Telmer, C. Tolg, J.B. McCarthy, E.A. Turley, How does a protein with dual mitotic spindle and extracellular matrix receptor functions affect tumor susceptibility and progression?, Communicative & integrative biology 4(2) (2011) 182-5.

Journal Pre-proof

[37] E.A. Turley, PURIFICATION OF A HYALURONATE-BINDING PROTEIN-FRACTION THAT MODIFIES CELL SOCIAL-BEHAVIOR, Biochemical and Biophysical Research Communications 108(3) (1982) 1016-1024.

[38] E.A. Turley, P.W. Noble, L.Y.W. Bourguignon, Signaling properties of hyaluronan receptors, J Biol Chem 277(7) (2002) 4589-4592.

[39] C.A. Maxwell, J. McCarthy, E. Turley, Cell-surface and mitotic-spindle RHAMM: moonlighting or dual oncogenic functions?, Journal of Cell Science 121(7) (2008) 925-932.

[40] I. Prudovsky, F. Tarantini, M. Landriscina, D. Neivandt, R. Soldi, A. Kirov, D. Small, K.M. Kathir, D. Rajalingam, T.K.S. Kumar, Secretion without Golgi, J. Cell. Biochem. 103(5) (2008) 1327-1343.

[41] C. Tolg, S.R. Hamilton, K.A. Nakrieko, F. Kooshesh, P. Walton, J.B. McCarthy, M.J. Bissell, E.A. Turley, Rhamm(-/-) fibroblasts are defective in CD44-mediated ERK1,2 motogenic signaling, leading to defective skin wound repair, Journal of Cell Biology 175(6) (2006) 1017-1028.

[42] S.R. Hamilton, S.F. Fard, F.F. Paiwand, C. Tolg, M. Veiseh, C. Wang, J.B. McCarthy, M.J. Bissell, J. Koropatnick, E.A. Turley, The hyaluronan receptors CD44 and Rhamm (CD168) form complexes with ERK1,2 that sustain high basal motility in breast cancer cells, J Biol Chem 282(22) (2007) 16667-16680.

[43] H. Hatano, H. Shigeishi, Y. Kudo, K. Higashikawa, K. Tobiume, T. Takata, N. Kamata, RHAMM/ERK interaction induces proliferative activities of cementifying fibroma cells through a mechanism based on the CD44-EGFR, Laboratory Investigation 91(3) (2011) 379-391.

[44] C. Tolg, S.R. Hamilton, L. Morningstar, J. Zhang, S. Zhang, K.V. Esguerra, P.G. Telmer, L.G. Luyt, R. Harrison, J.B. McCarthy, E.A. Turley, RHAMM Promotes Interphase Microtubule Instability and Mitotic Spindle Integrity through MEK1/ERK1/2 Activity, J Biol Chem 285(34) (2010) 26461-26474.

[45] M. Veiseh, D.H. Kwon, A.D. Borowsky, C. Tolg, H.S. Leong, J.D. Lewis, E.A. Turley, M.J. Bissell, Cellular heterogeneity profiling by hyaluronan probes reveals an invasive but slow-growing breast tumor subset, Proceedings of the National Academy of Sciences of the United States of America 111(17) (2014) E1731-E1739.

[46] J.S. Zhao, M. Yonede, M. Takeyama, O. Miyaishi, Y. Inoue, T. Kataoka, A. Ohno-Jinno, Z. Isogai, K. Kimata, M. Iwaki, M. Zako, Characterization of a motif for specific binding to hyaluronan in chicken SPACR, Journal of Neurochemistry 106(3) (2008) 1117-1124.

Journal Pre-proof

[47] B.H. Yang, B.L. Yang, R.C. Savani, E.A. Turley, Identification of a Common Hyaluronan-Binding Motif in the Hyaluronan-Binding Proteins Rhamm, Cd44 and Link Protein, Embo J 13(2) (1994) 286-296.

[48] T. Zal, N.R. Gascoigne, Photobleaching-corrected FRET efficiency imaging of live cells, Biophysical journal 86(6) (2004) 3923-3939.

[49] A.M. Carvalho, R. Teixeira, R. Novoa-Carballal, R.A. Pires, R.L. Reis, I. Pashkuleva, Redox-Responsive Micellar Nanoparticles from Glycosaminoglycans for CD44 Targeted Drug Delivery, Biomacromolecules 19(7) (2018) 2991-2999.

[50] L.Q. Chen, L.Y.W. Bourguignon, Hyaluronan-CD44 interaction promotes c-Jun signaling and miRNA21 expression leading to Bcl-2 expression and chemoresistance in breast cancer cells, Molecular Cancer 13 (2014).

[51] N. Sun, H.N. Xu, Q. Luo, L.Z. Li, Potential Indexing of the Invasiveness of Breast Cancer Cells by Mitochondrial Redox Ratios, Advances in experimental medicine and biology 923 (2016) 121-127.

[52] E.W. Thompson, S.M. Paik, N. Brunner, C.L. Sommers, G. Zugmaier, R. Clarke, T.B. Shima, J. Torri, S. Donahue, M.E. Lippman, G.R. Martin, R.B. Dickson, Association of increased basement-membrane invasiveness with absence of estrogen-receptor and expression of vimentin in human breast-cancer cell-lines, Journal of Cellular Physiology 150(3) (1992) 534-544.

[53] V. Assmann, J.F. Marshall, C. Fieber, M. Hofmann, I.R. Hart, The human hyaluronan receptor RHAMM is expressed as an intracellular protein in breast cancer cells, Journal of Cell Science 111 (1998) 1685-1694.

[54] C.A. Maxwell, J.J. Keats, A.R. Belch, L.M. Pilarski, T. Reiman, Receptor for hyaluronan-mediated motility correlates with centrosome abnormalities in multiple myeloma and maintains mitotic integrity, Cancer Research 65(3) (2005) 850-860.

[55] S. Sohr, K. Engeland, RHAMM is differentially expressed in the cell cycle and downregulated by the tumor suppressor p53, Cell Cycle 7(21) (2008) 3448-3460.

[56] S. Nedvetzki, E. Gonen, N. Assayag, R. Reich, R.O. Williams, R.L. Thurmond, J.F. Huang, B.A. Neudecker, F.S. Wang, E.A. Turley, D. Naor, RHAMM, a receptor for hyaluronan-mediated motility, compensates for CD44 in inflamed CD44-knockout mice: A different interpretation of redundancy, Proceedings of the National Academy of Sciences of the United States of America 101(52) (2004) 18081-18086.

Journal Pre-proof

[57] R. Novoa-Carballal, C. Silva, S. Moller, M. Schnabelrauch, R.L. Reis, I. Pashkuleva, Tunable nano-carriers from clicked glycosaminoglycan block copolymers, Journal of Materials Chemistry B 2(26) (2014) 4177-4184.

[58] N. Altgarde, E. Nileback, L. de Battice, I. Pashkuleva, R.L. Reis, J. Becher, S. Moller, M. Schnabelrauch, S. Svedhem, Probing the biofunctionality of biotinylated hyaluronan and chondroitin sulfate by hyaluronidase degradation and aggrecan interaction, Acta Biomaterialia 9(9) (2013) 8158-8166.

[59] D.J. Aguiar, W. Knudson, C.B. Knudson, Internalization of the hyaluronan receptor CD44 by chondrocytes, Exp Cell Res 252(2) (1999) 292-302.

[60] R.B. Sekar, A. Periasamy, Fluorescence resonance energy transfer (FRET) microscopy imaging of live cell protein localizations, Journal of Cell Biology 160(5) (2003) 629-633.

[61] S.R. Hamilton, S.F. Fard, F.F. Paiwand, C. Tolg, M. Veiseh, C. Wang, J.B. McCarthy, M.J. Bissell, J. Koropatnick, E.A. Turley, The hyaluronan receptors CD44 and Rhamm (CD168) form complexes with ERK1,2 that sustain high basal motility in breast cancer cells, The Journal of biological chemistry 282(22) (2007) 16667-16680.

[62] C. Yang, M. Cao, Y. Liu, Y. He, Y. Du, G. Zhang, F. Gao, Inducible formation of leader cells driven by CD44 switching gives rise to collective invasion and metastases in luminal breast carcinomas, Oncogene 38(46) (2019) 7113-7132.

[63] S.W. Zhang, M.C.Y. Chang, D. Zylka, S. Turley, R. Harrison, E.A. Turley, The hyaluronan receptor RHAMM regulates extracellular-regulated kinase, J Biol Chem 273(18) (1998) 11342-11348.

[64] D. Park, Y. Kim, H. Kim, K. Kim, Y.S. Lee, J. Choe, J.H. Hahn, H. Lee, J. Jeon, C. Choi, Y.M. Kim, D. Jeoung, Hyaluronic acid promotes angiogenesis by inducing RHAMM-TGF beta receptor interaction via CD44-PKC delta, Molecules and Cells 33(6) (2012) 563-574.

[65] D. Nikitovic, K. Kouvidi, N.K. Karamanos, G.N. Tzanakakis, The Roles of Hyaluronan/RHAMM/CD44 and Their Respective Interactions along the Insidious Pathways of Fibrosarcoma Progression, Biomed Research International (2013).

[66] Y.C.N. Du, C.K. Chou, D.S. Klimstra, H. Varmus, Receptor for hyaluronan-mediated motility isoform B promotes liver metastasis in a mouse model of multistep tumorigenesis and a tail vein assay for metastasis, Proceedings of the National Academy of Sciences of the United States of America 108(40) (2011) 16753-16758.

Journal Pre-proof

[67] R.C. Savani, G.Y. Cao, P.M. Pooler, A. Zaman, Z. Zhou, H.M. DeLisser, Differential involvement of the hyaluronan (HA) receptors CD44 and receptor for HA-mediated motility in endothelial cell function and angiogenesis, J Biol Chem 276(39) (2001) 36770-36778.

[68] D. Manzanares, M.E. Monzon, R.C. Savani, M. Salathe, Apical oxidative hyaluronan degradation stimulates airway ciliary beating via RHAMM and RON, American Journal of Respiratory Cell and Molecular Biology 37(2) (2007) 160-168.

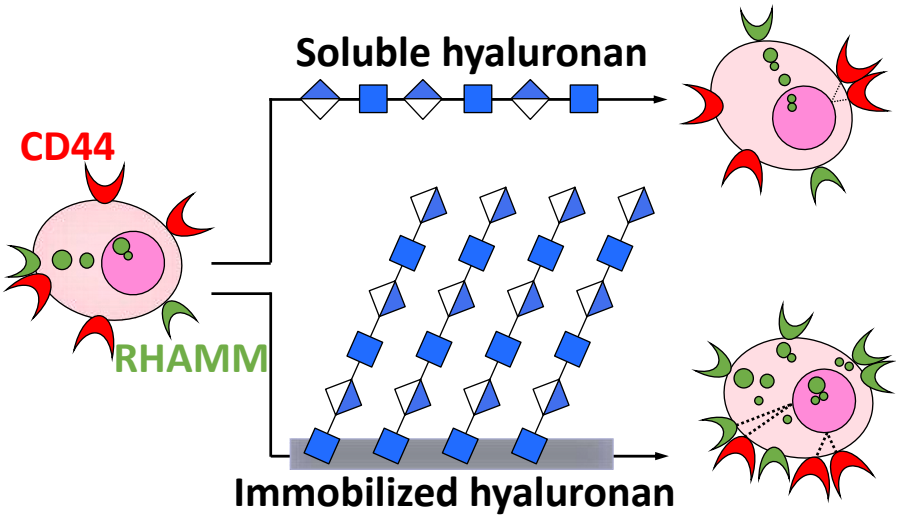
[69] I. Okamoto, Y. Kawano, H. Tsuiki, J. Sasaki, M. Nakao, M. Matsumoto, M. Suga, M. Ando, M. Nakajima, H. Saya, CD44 cleavage induced by a membrane-associated metalloprotease plays a critical role in tumor cell migration, Oncogene 18(7) (1999) 1435-1446.

[70] L.A. Gurski, X. Xu, L.N. Labrada, N.T. Nguyen, L.X. Xiao, K.L. van Golen, X.Q. Jia, M.C. Farach-Carson, Hyaluronan (HA) Interacting Proteins RHAMM and Hyaluronidase Impact Prostate Cancer Cell Behavior and Invadopodia Formation in 3D HA-Based Hydrogels, Plos One 7(11) (2012).

[71] B.D. Lynn, X.B. Li, P.A. Cattini, J.I. Nagy, Sequence, protein expression and extracellular-regulated kinase association of the hyaladherin RHAMM (receptor for hyaluronan mediated motility) in PC12 cells, Neuroscience Letters 306(1-2) (2001) 49-52.

Journal Pre-proof

Table of Contents Graphic:



Journal Pre-proof